Reviews of Geophysics

Supporting Information for

Climatic changes and their elevational patterns in the mountains of the world

N.C. Pepin[1], E. Arnone[2,6], A. Gobiet[3], K. Haslinger[3], S. Kotlarski[4], C. Notarnicola[5], E. Palazzi[6], P. Seibert[7], S. Serafin[8], W. Schöner[9], S. Terzago[6], J.M. Thornton[10], M. Vuille[11] and C. Adler[10]

[1] School of Environment, Geography and Geoscience, University of Portsmouth, U.K.

[2] Department of Physics, University of Torino, Torino, Italy

[3]Climate Research Department, Central Institute for Meteorology and Geodynamics (ZAMG), Vienna, Austria

[4] Federal Office of Meteorology and Climatology, Meteo Swiss, Zurich, Switzerland

[5] EURAC Institute for Earth Observation, Bolzano, Italy

[6] National Research Council of Italy, Institute of Atmospheric Sciences and Climate (CNR-ISAC), Torino, Italy

[7] Institute of Meteorology and Climatology, University of Natural Resources and Life Sciences, Vienna, Austria

[8] Dept of Meteorology and Geophysics, University of Vienna, Vienna, Austria

[9]Institute of Geography and Regional Science, University of Graz, Austria

[10] Mountain Research Initiative, University of Bern, Switzerland

[11]Department of Atmospheric and Environmental Sciences, University at Albany, Albany, NY, USA

]

Contents of this file

Tables S1 to S3
Text T1 to T4

Introduction

This file contains information as follows

Table S1: List of CMIP5 models followed by references Text T1

Text T2: Details of observational datasets

Text T3: Metadata on SROCC station analyses

Text T4: List of references from SROCC Tables

Tables S2 and S3: Detailed regional trends in temperature and precipitation

Model ID	**Resolution Lon × Lat° Lev**	**Institution ID**	**Key reference**
ACCESS1-0	**1.875 × 1.25L38 (N96)**	**CSIRO-BOM**	**Bi et al. (2013)**
ACCESS1-3	**1.875 × 1.25L38**	**CSIRO-BOM**	**Bi et al. (2013)**
bcc-csm1-1-m	**1.125 × 1.125L26 (T106)**	**BCC**	**Wu et al. (2013)**
bcc-csm1-1	**2.8125 × 2.8125L26 (T42)**	**BCC**	**Wu et al. (2013)**
BNU-ESM	**2.8125 × 2.8125L26 (T42)**	**BNU**	**Ji et al. (2014)**
CanESM2	**2.8125 × 2.8125L35 (T63)**	**CCCMA**	**Arora et al. (2011)**
CCSM4	**1.25 × 0.9L27 (T63)**	**NCAR**	**Meehl et al. (2012)**
CESM1-BGC	**1.25 × 0.9L27**	**NSF-DOE-NCAR**	**Hurrell et al. (2013)**
CESM1-CAM5	**1.25 × 0.9L27**	**NSF-DOE-NCAR**	**Hurrell et al. (2013)**
CESM1-FASTCHEM	**1.25 × 0.9L27**	**NSF-DOE-NCAR**	**Hurrell et al. (2013)**
CESM1-WACCM	**2.5 × 1.9**	**NSF-DOE-NCAR**	**Hurrell et al. (2013)**
CMCC-CESM	**3.75 x 3.75**	**CMCC**	**Hurrell et al. (2013)**
CMCC-CM	**0.75 × 0.75L31 (T159)**	**CMCC**	**Scoccimarro et al. (2011)**
CMCC-CMS	**1.875 × 1.875L95 (T63)**	**CMCC**	**Davini et al. (2013)**
CNRM-CM5	**1.40625 × 1.40625L31 (T127)**	**CNRM-CERFACS**	**Voldoire et al. (2013)**
CNRM-CM5-2	**1.40625 × 2.8125**	**CNRM-CERFACS**	**Voldoire et al. (2013)**
CSIRO-Mk3-6-0	**1.875 × 1.875L18 (T63)**	**CSIRO-QCCCE**	**Rotstayn et al. (2012)**
EC-Earth	**1.125 × 1.125L62 (T159)**	**EC-EARTH**	**Hazeleger et al. (2012)**
FGOALS-g2	**2.8125 × 2.8125L26**	**LASG-CESS**	**Li et al. (2013)**
FIO-ESM	**2.8125 × 2.8125L26 (T42)**	**FIO**	**Song et al. (2012)**

GFDL-ESM2G	**2.5 × 2L24 (M45)**	**GFDL**	**Delworth et al. (2006)**
GFDL-ESM2M	**2.5 × 2L24 (M45)**	**GFDL**	**Delworth et al. (2006)**
GFDL-CM2p1	**2.5 × 2L24 (M45)**	**GFDL**	**Yang et al. (2020)**
GFDL-CM3	**2.5 × 2L48 (C48)**	**GFDL**	**Delworth et al. (2006)**
GISS-E2-H-CC	**2×2.5×L40**	**NASA GISS**	**Miller et al. (2014)**
GISS-E2-R-CC	**2×2.5×L40**	**NASA GISS**	**Miller et al. (2014)**
GISS-E2-R	**2×2.5×L40**	**NASA GISS**	**Miller et al. (2014)**
HadCM3	**3.75 x 2.5(L19)**	**MOHC**	**Johns et al. (2003)**
HadGEM2-AO	**1.875 × 1.24L60**	**MOHC**	**Martin et al. (2011)**
HadGEM2-CC	**1.875 × 1.24L60 (N96)**	**MOHC**	**Martin et al. (2011)**
HadGEM2-ES	**1.875 × 1.24L38 (N96)**	**MOHC**	**Bellouin et al. (2011)**
INM-CM4	**2 × 1.5L21**	**INM**	**Volodin et al. (2010)**
IPSL-CM5A-LR	**3.75 × 1.89L39**	**IPSL**	**Hourdin et al. (2013)**
IPSL-CM5A-MR	**2.5 × 1.2587L39**	**IPSL**	**Hourdin et al. (2013)**
IPSL-CM5B-LR	**3.75 × 1.9L39**	**IPSL**	**Hourdin et al. (2013)**
MIROC5	**1.40625 × 1.40625L40 (T85)**	**MIROC**	**Watanabe et al. (2010)**
MIROC-ESM	**2.8125 × 2.8125L80 (T42)**	**MIROC**	**Watanabe et al. (2011)**
MIROC-ESM-CHEM	**2.8125 × 2.8125L80 (T42)**	**MIROC**	**Watanabe et al. (2011)**
MPI-ESM-LR	**1.875 × 1.875L47 (T63)**	**MPI-M**	**Giorgetta et al. (2013)**
MPI-ESM-MR	**1.875 × 1.875L95 (T63)**	**MPI-M**	**Giorgetta et al. (2013)**
MPI-ESM-P	**1.875 × 1.875 (T63)**	**MPI**	**Giorgetta et al. (2013)**
MRI-CGCM3	**1.125 × 1.125L48 (T159)**	**MRI**	**Yukimoto et al. (2012)**
NorESM1-M	**2.5 × 1.9L26 (F19)**	**NCC**	**Bentsen et al. (2013)**
NorESM1-ME	**2.5 × 1.9L26**	**NCC**	**Bentsen et al. (2013)**

Table S1: List of CMIP5 models used to create the model ensemble in this study.

Text T1: References for Table S1

Arora, V. K., Scinocca, J. F., Boer, G. J., Christian, J. R., Denman, K. L., Flato, G. M., Kharin, V. V., Lee, W. G. & Merryfield, W. J. (2011). Carbon emission limits required to satisfy future representative concentration pathways of greenhouse gases. *Geophysical Research Letters*, 38(5), https://doi.org/10.1029/2010GL046270.

Bellouin, N., Rae, J., Jones, A., Johnson, C., Haywood, J., & Boucher, O. (2011b). Aerosol forcing in the Climate Model Intercomparison Project (CMIP5) simulations by HadGEM2-ES and the role of ammonium nitrate. *Journal of Geophysical Research: Atmospheres*, *116*(D20), https://doi.org/10.1029/2011JD016074.

Bentsen, M., Bethke, I., Debernard, J. B., Iversen, T., Kirkevåg, A., Seland, Ø., Drange, H., Roelandt, C., Seierstad, I. A., Hoose, C. & Kristjansson, J. E. (2013). The Norwegian Earth System Model, NorESM1-M–Part 1: description and basic evaluation of the physical climate. *Geosci. Model Dev*., 6, 687–720, https://doi.org/10.5194/gmd-6-687-2013.

Bi, D., Dix, M., Marsland, S. J., O'Farrell, S., Rashid, H., Uotila, P., Hirst, A., Kowalczyk, E., Golebiewski, M., Sullivan, A., Yan, H., Hannah, N., Franklin, C., Sun, Z., Vohralik, P., Watterson, I., Zhou, X., Fiedler, R., Collier, M., Ma, Y., Noonan, J., Stevens, L., Uhe, P., Zhu, H., Griffies, S., Hill, R., Harris, C., & Puri, K. (2013). The ACCESS coupled model: description, control climate and evaluation. *Aust. Meteorol. Oceanogr. J*, *63*(1), 41-64, https://doi.org/10.22499/2.6301.004.

Davini, P., Cagnazzo, C., Fogli, P. G., Manzini, E., Gualdi, S., & Navarra, A. (2014). European blocking and Atlantic jet stream variability in the NCEP/NCAR reanalysis and the CMCC-CMS climate model. *Climate dynamics*, *43*(1-2), 71-85, https://doi.org/10.1007/s00382-013-1873-y.

Delworth, T. L., Broccoli, A. J., Rosati, A., Stouffer, R. J., Balaji, V., Beesley, J. A., Cooke, W. F., Dixon, K., Dunne, J., Dunne, K. A., Durachta, J. W., Findell, K. L., Ginoux, P., Gnanadesikan, A., Gordon, C. T., Griffies, S. M., Gudgel, R., Harrison, M. J., Held, I. M., Hemler, R. S., Horowitz, L. W., Klein, S. A., Knutson, T. R., Kushner, P. J., Langenhorst, A. R., Lee, H. C., Lin, S. J., Lu, J., Malyshev, S. L., Milly, P. C. D., Ramaswamy, V., Russell, J., Schwarzkopf, M. D., Shevliakova, E., Sirutis, J. J., Spelman, M. J., Stern, W. F., Winton, M., Wittenberg, A. T., Wyman, B., Zeng. F., & Zhang, R. (2006). GFDL's CM2 global coupled climate models. Part I: Formulation and simulation characteristics. *Journal of Climate*, *19*(5), 643-674, https://doi.org/10.1175/JCLI3629.1.

Giorgetta, M. A., Jungclaus, J., Reick, C. H., Legutke, S., Bader, J., Böttinger, M., Brovkin, V., Crueger, T., Esch, M., Fieg, K., Glushak, K., Gayler, V., Haak, H., Hollweg, H. D., Ilyina, T., Kinne, S., Kornblueh, L., Matei, D., Mauritsen, T., Mikolajewicz, U., Mueller, W., Notz, D., Pithan, F., Raddatz, T., Rast, S., Redler, R., Roeckner, E., Schmidt, H., Schnur, R., Segschneider, J., Six, K. D., Stockhause, M., Timmreck, C., Wegner, J., Widmann, H., Wieners, K. H., Claussen, M., Marotzke, J., & Stevens, B. (2013). Climate and carbon cycle changes from 1850 to 2100 in MPI-ESM simulations for the Coupled Model Intercomparison Project phase 5. *Journal of Advances in Modeling Earth Systems*, *5*(3), 572-597, https://doi.org/10.1002/jame.20038.

Hazeleger, W., Wang, X., Severijns, C., Ştefãnescu, S., Bintanja, R., Sterl, A., Wyser, K., Semmler, T., Yang, S., van den Hurk, B., van Noije, T., van der Linden, E., Van der Wiel, K. (2012). EC-Earth V2. 2: description and validation of a new seamless earth system prediction model. *Climate dynamics*, *39*(11), 2611-2629, https://doi.org/10.1007/s00382-011-1228-5.

Hourdin, F., Foujols, M. A., Codron, F., Guemas, V., Dufresne, J. L., Bony, S., Denvil, S., Guez, L., Lott, F., Ghattas, J., Braconnot, P., Marti, O., Meurdesoif, Y., & Bopp, L. (2013). Impact of the LMDZ atmospheric grid configuration on the climate and sensitivity of the IPSL-CM5A coupled model. *Climate Dynamics*, 40(9-10), 2167-2192, https://doi.org/10.1007/s00382-012-1411-3.

Hurrell, J. W., Holland, M. M., Gent, P. R., Ghan, S., Kay, J. E., Kushner, P. J., Lamarque, J. F., Large, W. G., Lawrence, D., Lindsay, K., Lipscomb, W. H., Long, M. C., Mahowald, N., Marsh, D. R., Neale, R. B., Rasch, P., Vavrus, S., Vertenstein, M., Bader, D., Collins, W. D., Hack, J. J., Kiehl, J. & Marshall, S. (2013). The community earth system model: a framework for collaborative research. *Bulletin of the American Meteorological Society*, 94(9), 1339-1360, https://doi.org/10.1175/BAMS-D-12-00121.1.

Ji, D., Wang, L., Feng, J., Wu, Q., Cheng, H., Zhang, Q., Yang, J., Dong, W., Dai, Y., Gong, D., Zhang, R.-H., Wang, X., Liu, J., Moore, J. C., Chen, D., & Zhou, M. (2014). Description and basic evaluation of Beijing Normal University Earth System Model (BNU-ESM) version 1, *Geosci. Model Dev*., 7, 2039–2064, https://doi.org/10.5194/gmd-7-2039-2014.

Johns, T. C., Gregory, J. M., Ingram, W. J., Johnson, C. E., Jones, A., Lowe, J. A., Mitchell, J. F. B., Roberts, D. L., Sexton, D. M. H. , Stevenson, D. S. , Tett, S. F. B. & Woodage, M. J. (2013). Anthropogenic climate change for 1860 to 2100 simulated with the HadCM3 model under updated emissions scenarios. *Climate Dynamics*, 20, 583–612, https://doi.org/10.1007/s00382-002-0296-y

Li, L., Lin, P., Yu, Y., Wang, B., Zhou, T., Liu, L., Liu. J., Bao, Q., Xu, S., Huang, W., Xia, K., Pu, Y., Dong, L., Shen, S., Liu, Y., Hu, N., Liu, M., Sun, W., Shi, X., Zheng, W., Wu, B., Song, M., Liu, H., Zhang, X., Wu, G., Xue, W., Huang, X., Yang, G., Song, Z., & Qiao, F. (2013). The flexible global ocean-atmosphere-land system model, Grid-point Version 2: FGOALS-g2. *Advances in Atmospheric Sciences*, 30(3), 543-560, https://doi.org/10.1007/s00376-012-2140-6.

Martin, G. M., Bellouin, N., Collins, W. J., Culverwell, I. D., Halloran, P. R., Hardiman, S. C., Hinton, T. J., Jones, C. D., McDonald, R. E., McLaren, A. J., O'Connor, F. M., Roberts, M. J., Rodriguez, J. M., Woodward, S., Best, M. J., Brooks, M. E., Brown, A. R., Butchart, N., Dearden, C., Derbyshire, S. H., Dharssi, I., Doutriaux-Boucher, M., Edwards, J. M., Falloon, P. D., Gedney, N., Gray, L. J., Hewitt, H. T., Hobson, M., Huddleston, M. R., Hughes, J., Ineson, S., Ingram, W. J., James, P. M., Johns, T. C., Johnson, C. E., Jones, A., Jones, C. P., Joshi, M. M., Keen, A. B., Liddicoat, S., Lock, A.

P., Maidens, A. V., Manners, J. C., Milton, S. F., Rae, J. G. L., Ridley, J. K., Sellar, A., Senior, C. A., Totterdell, I. J., Verhoef, A., Vidale, P. L., and Wiltshire, A. (2011). The HadGEM2 family of Met Office Unified Model climate configurations. *Geosci. Model Dev*., 4, 723–757, https://doi.org/10.5194/gmd-4-723-2011.

Meehl, G. A., Washington, W. M., Arblaster, J. M., Hu, A., Teng, H., Tebaldi, C., Strand, W. G., & White III, J. B. (2012). Climate system response to external forcings and climate change projections in CCSM4. *Journal of Climate*, 25(11), 3661-3683, https://doi.org/10.1175/JCLI-D-11-00240.1.

Miller, R. L., Schmidt, G. A., Nazarenko, L. S., Tausnev, N., Bauer, S. E., Del Genio, A. D., Kelley, M., Lo, K. K., Ruedy, R., Shindell, D. T., Aleinov, I., Bauer, M., Bleck, R., Canuto, V., Chen, Y., Cheng, Y., Clune, T. L., Faluvegi, G., Hansen, J. E., Healy, R.J. , Kiang, N.Y., Koch, D., Lacis, A. A., LeGrande, A. N., Lerner, J., Menon, S., Oinas, V., Perez Garca-Pando, C., Perlwitz, J. P., Puma, M. J., Rind, D., Romanou, A., Russell, G. L., Sato, Mki., Sun, S., Tsigaridis, K., Unger, N., Voulgarakis, A., Yao, M.-S. & Zhang, J. (2014). CMIP5 historical simulations (1850-2012) with GISS ModelE2. *J. Adv. Model. Earth Syst*., 6, no. 2, 441-477, https://doi.org/10.1002/2013MS000266.

Rotstayn, L.D., Jeffrey, S. J., Collier, M. A., Dravitzki, S. M., Hirst, A. C., Syktus, J. I., Wong, K. K. (2012). Aerosol-and greenhouse gas- induced changes in summer rainfall and circulation in the Australasian region: a study using single-forcing climate simulations. *Atmos Chem Phys* 12:6377–6404, https://doi.org/10.5194/acp-12-6377-2012.

Scoccimarro, E., Gualdi, S., Bellucci, A., Sanna, A., Fogli, P. G., Manzini, E., Vichi, M., Oddo, P., Navarra, A. (2011). Effects of tropical cyclones on ocean heat transport in a high resolution coupled general circulation model. J Clim 24:4368–4384, https://doi.org/10.1175/2011JCLI4104.1.

Song, Z., Qiao, F., Song, Y. (2012), Response of the equatorial basin-wide SST to wave mixing in a climate model: an amendment to tropical bias. *J Geophys Res* 117:C00J26, https://doi.org/10.1029/2012JC007931.

Voldoire, A., Sanchez-Gomez, E., y Mélia, D. S., Decharme, B., Cassou, C., Sénési, S., Valcke, S., Beau, I., Alias, A., Chevallier, M,, Déqué, M., Deshayes, J., Douville, H., Fernandez, E., Madec, G., Maison- nave, E., Moine, M. P., Planton, S., Saint-Martin, D., Szopa, S., Tyteca, S., Alkama, R., Belamari, S., Braun, A., Coquart, L., Chauvin, F. (2013). The CNRM-CM5.1 global climate model: description and basic evaluation. *Clim Dyn* 40:2091–2121, https://doi.org/10.1007/s00382-011-1259-y.

Volodin, E. M., Dianskii, N. A., Gusev, A. V. (2010). Simulating present-day climate with the INMCM4.0 coupled model of the atmospheric and oceanic general circulations. *Izv Atmos Ocean Phys* 46:414– 431, https://doi.org/10.1134/S000143381004002X.

Watanabe, M., Suzuki, T., O'ishi, R., Komuro, Y., Watanabe, S., Emori, S., Takemura, T., Chikira, M., Ogura, T., Sekiguchi, M., Takata, K., Yamazaki, D., Yokohata, T., Nozawa, T., Hasumi, H., Tatebe, H., & Kimoto, M. (2010). Improved Climate Simulation by MIROC5: Mean States, Variability, and Climate Sensitivity, *Journal of Climate*, *23*(23), 6312-6335, https://doi.org/10.1175/2010JCLI3679.1.

Watanabe, S., Hajima, T., Sudo, K., Nagashima, T., Takemura, T., Okajima, H., Nozawa, T., Kawase, H., Abe, M., Yokohata, T., Ise, T., Sato, H., Kato, E., Takata, K., Emori, S., Kawamiya, M. (2011). MIROC- ESM 2010: model description and basic results of CMIP5- 20c3m experiments. *Geosci Model Dev* 4:845–872, https://doi.org/10.5194/gmd-4-845-2011.

Wu, T., Li, W., Ji, J., Xin, X., Li, L., Wang, Z., Zhang, Y., Li, J., Zhang, F., Wei, M., Shi, X., Wu, F., Zhang, L., Chu, M., Jie, W., Liu, Y., Wang, F., Liu, X., Li, Q., Dong, M., Liang, X., Gao, Y., Zhang, J. (2013). Global carbon budgets simulated by the Beijing Climate Center climate system model for the last century. J *Geophys Res Atmos* 118:4326–4347, https://doi.org/10.1002/jgrd.50320.

Yang, Z., Fang, X. & Mu, Mu. (2020). The Optimal Precursor of El Niño in the GFDL CM2p1 Model. *Journal of Geophysical Research: Oceans*, 125, https://doi.org/10.1029/2019JC015797.

Yukimoto, S., Adachi, Y., Hosaka, M., Sakami, T., Yoshimura, H., Hirabara, M., Tanaka, T. Y., Shindo, E., Tsujino, H., Deushi, M., Mizuta, R., Yabu, S., Obata, A., Nakano, H., Koshiro, T., Ose, T., Kitoh, A. (2012). A new global climate model of the Meteorological Research Institute: MRI-CGCM3—model description and basic performance. *J Meteorol Soc Jpn* Ser II 90A:23–64, https://doi.org/10.2151/jmsj.2012-A02.

Text: T2: Descriptions of Gridded Datasets used in this study

The Climatic Research Unit gridded Time Series (**CRU TS**) dataset (Harris et al., 2020) is a high-resolution (0.5°x0.5°) monthly gridded database of station observations with global coverage (land-only, excluding Antarctica) covering 1901-2018. It provides both near surface temperature (K) and total precipitation (mm/month) based on over 4,000 stations (10,000 since the 1970s). Observations from individual stations are normalized to their 1961-1990 mean, gridded to the regular grid using angular distance weighting, and resulting anomalies converted to absolute values using the CRU CL v1.0 climatology. Synthesized observations (at 2.5° resolution) are used to fill gaps in regions of poor observational coverage.

The GISS Surface Temperature (**GISTEMP**) dataset provides monthly estimates of global surface temperature anomalies covering the time period 1880-2019 over a grid of 2x2°latitude-longitude resolution. The version employed in this study is GISTEMP v4 (with a 250 km smoothing radius, i.e. the distance in kilometers over which a station influences regional temperature (Hansen et al., 2010, Lenssen et al., 2019).

The Global Precipitation Climatology Centre (**GPCC**) reanalysis is a precipitation gridded dataset based on gauge measurements. It is particularly recommended for model verification and for analysis of historic global precipitation, or for research on the global water cycle (Becker et al. 2013, Schneider et al. 2017). GPCC version 2018 data extend from 1901 to 2018 and consist of monthly precipitation at 0.25°x0.25° spatial resolution. The data coverage per month varies from ~10,000 stations at the beginning of the 20th century to more than 45,000 stations in 1986/1987. For further details about the spatial distribution of the stations underlying the GPCC dataset see Schneider et al. (2017). The GPCC monthly precipitation anomalies are spatially interpolated using a spherical adaptation of Shepard's empirical weighting scheme. The latest version also includes estimates of the mean systematic gauge-error.

ERA5 is the latest reanalysis dataset of the European Centre for Medium-Range Weather Forecasts (Hersbach et al., 2020). It largely improves on the previously widely adopted ERA-Interim data in terms of resolution and physics. It merges information from a vast range of observations with models and assimilation techniques into a global 0.25°x0.25° dataset, covering 1979 to present at the time of compiling this article. The newest version includes information on uncertainty through an ensemble approach. A very recent extension back to 1950 was not used.

An ensemble of **Global climate and Earth system models** from the Coupled Model Intercomparison Project Phase 5 (hereafter **CMIP5**) were considered in this study. We adopted temperature and precipitation output of historical (1900–2005) simulations of 32 models from the CMIP5 project (Taylor et al., 2012) available from the Earth System Grid Federation archive data portal (http://esgf.llnl.gov). The full list of models is reported in Table S1. The models are based on a variety of spatial resolutions (from 0.75° to 2.8°) and various degrees of sophistication (e.g. biogeochemical cycles, interactive aerosol, cloud-aerosol interaction). Further model details and information on their configuration or features can be found in the PCMDI data portal (http:// www-pcmdi.llnl.gov/) and in Chapter 9 of the 5th IPCC Assessment Report (AR5, IPCC 2013). Model data were first re-gridded to a common 1°x1° reference grid and then averaged to obtain the multi-model mean. Only one ensemble member per model was considered (the *r1i1p1* if available). Although CMIP6 models have just been released, CMIP5 models have been thoroughly tested and broadly used in a vast range of studies and can therefore represent the best well-documented choice for this study (e.g., IPCC 2013).

References are listed in the main text.

Text: T3: Metadata concerning highlighted values in Table 1 (main text)

All values are converted to ˚C/decade

Qixiang et al. (2018). IPCC SROCC says +0.40/+0.35 but the original literature calculates +0.43 for the high elevation warming rate which is 2.165/5.

Oyler et al. (2015) The trend given in the abstract, based on the primary analysis and corrections applied in the paper is for 1991-2012 and we use this figure (+0.11)

Ceppi et al. (2012) The figure given in the abstract is +0.48 (not +0.46 as in SROCC). This is contradicted later in the article so there is a discrepancy.

Yan et al. (2014) Appears to be missing from the final SROCC table, but was included in earlier drafts and so is included here.

Text: T4: References from meta-study (Table 1 in main text and Tables SM2.2 and SM2.4 in SROCC)

Archer, D. R., & Fowler, H. J. (2004). Spatial and temporal variations in precipitation in the Upper Indus Basin, global teleconnections and hydrological implications. *Hydrology and Earth System Sciences*, *8*(1), 47–61. https://doi.org/10.5194/hess-8-47-2004

Begert, M., & Frei, C. (2018). Long-term area-mean temperature series for Switzerland-Combining homogenized station data and high resolution grid data. *International Journal of Climatology*, *38*(6), 2792–2807. https://doi.org/10.1002/joc.5460

Bhutiyani, M. R., Kale, V. S., & Pawar, N. J. (2007). Long-term trends in maximum, minimum and mean annual air temperatures across the Northwestern Himalaya during the twentieth century. *Climatic Change*, *85*(1–2), 159–177. https://doi.org/10.1007/s10584-006-9196-1

Bhutiyani, M. R., Kale, V. S., & Pawar, N. J. (2010). Climate change and the precipitation variations in the northwestern Himalaya: 1866-2006. *International Journal of Climatology*, *30*(4), 535–548. https://doi.org/10.1002/joc.1920

Caloiero, T. (2015). Analysis of rainfall trend in New Zealand. *Environmental Earth Sciences*, *73*(10), 6297–6310. https://doi.org/10.1007/s12665-014-3852-y

Ceppi, P., Scherrer, S. C., Fischer, A. M., & Appenzeller, C. (2012). Revisiting Swiss temperature trends 1959-2008. *International Journal of Climatology*, *32*(2), 203–213. https://doi.org/10.1002/joc.2260

Chen, Y., Li, W., Deng, H., Fang, G., & Li, Z. (2016). Changes in Central Asia's Water Tower: Past, Present and Future. *Scientific Reports*, *6*(1), 35458. https://doi.org/10.1038/srep35458

Crochet, P. (2007). A Study of Regional Precipitation Trends in Iceland Using a High-Quality Gauge Network and ERA-40. *Journal of Climate*, *20*(18), 4659–4677. https://doi.org/10.1175/JCLI4255.1

Deng, H., Pepin, N. C., & Chen, Y. (2017). Changes of snowfall under warming in the Tibetan Plateau. *Journal of Geophysical Research: Atmospheres*, *122*(14), 7323–7341. https://doi.org/10.1002/2017JD026524

Diaz, H. F., & Bradley, R. S. (1997). Temperature variations during the last century at high elevation sites. *Climatic Change*, *36*(1990), 253–279. https://doi.org/10.1007/978-94-015-8905-5_2

Diaz, H. F., Eischeid, J. K., Duncan, C., & Bradley, R. S. (2003). Variability of Freezing Levels, Melting Season Indicators, and Snow Cover for Selected High-Elevation and Continental Regions in the Last 50 Years. *Climatic Change*, (1996), 33–52. https://doi.org/10.1007/978-94-015-1252-7_3

Dimri, A. P., & Dash, S. K. (2012). Wintertime climatic trends in the western Himalayas. *Climatic Change*, *111*(3–4), 775–800. https://doi.org/10.1007/s10584-011-0201-y

Elizbarashvili, M., Elizbarashvili, E., Tatishvili, M., Elizbarashvili, S., Meskhia, R., Kutaladze, N., et al. (2017). Georgian climate change under global warming conditions. *Annals of Agrarian Science*, *15*(1), 17–25. https://doi.org/10.1016/j.aasci.2017.02.001

Fujibe, F., Yamazaki, N., Katsuyama, M., & Kobayashi, K. (2005). The Increasing Trend of Intense Precipitation in Japan Based on Four-hourly Data for a Hundred Years. *SOLA*, *1*, 41–44. https://doi.org/10.2151/sola.2005-012

Gao, Y., Xu, J., & Chen, D. (2015). Evaluation of WRF mesoscale climate simulations over the Tibetan Plateau during 1979-2011. *Journal of Climate*, *28*(7), 2823–2841. https://doi.org/10.1175/JCLI-D-14-00300.1

Gilbert, A., & Vincent, C. (2013). Atmospheric temperature changes over the 20th century at very high elevations in the European Alps from englacial temperatures. *Geophysical Research Letters*, *40*(10), 2102–2108. https://doi.org/10.1002/grl.50401

Grose, M., Abbs, D., Bhend, J., Chiew, F. H. S., Church, J., Ekstrom, M., et al. (2015). *Southern Slopes Cluster Report*. *Climate Change in Australia Projections for Australia's Natural Resource Management Regions: Cluster Reports*.

Guo, D., Wang, H., & Li, D. (2012). A projection of permafrost degradation on the Tibetan Plateau during the 21st century. *Journal of Geophysical Research: Atmospheres*, *117*(D5), n/a-n/a. https://doi.org/10.1029/2011JD016545

Hammad, A. A., & Salameh, A. M. (2019). Temperature analysis as an indicator of climate change in the Central Palestinian Mountains. *Theoretical and Applied Climatology*, *136*(3–4), 1453–1464. https://doi.org/10.1007/s00704-018-2561-y

Irannezhad, M., Ronkanen, A.-K., Kiani, S., Chen, D., & Kløve, B. (2017). Long-term variability and trends in annual snowfall/total precipitation ratio in Finland and the role of atmospheric circulation patterns. *Cold Regions Science and Technology*, *143*, 23–31. https://doi.org/10.1016/j.coldregions.2017.08.008

Kormann, C., Francke, T., Renner, M., & Bronstert, A. (2015). Attribution of high resolution streamflow trends in Western Austria – an approach based on climate and discharge station data. *Hydrology and Earth System Sciences*, *19*(3), 1225–1245. https://doi.org/10.5194/hess-19-1225-2015

Krishnan, R., Shrestha, A. B., Ren, G., Rajbhandari, R., Saeed, S., Sanjay, J., et al. (2019). Unravelling Climate Change in the Hindu Kush Himalaya: Rapid Warming in the Mountains and Increasing Extremes. In *The Hindu Kush Himalaya Assessment* (pp. 57–97). Cham: Springer International Publishing. https://doi.org/10.1007/978-3-319-92288-1_3

Krishnaswamy, J., John, R., & Joseph, S. (2014). Consistent response of vegetation dynamics to recent climate change in tropical mountain regions. *Global Change Biology*, *20*(1), 203–215. https://doi.org/10.1111/gcb.12362

Lejeune, Y., Dumont, M., Panel, J.-M., Lafaysse, M., Lapalus, P., Le Gac, E., et al. (2019). 57 years (1960–2017) of snow and meteorological observations from a mid-altitude mountain site (Col de Porte, France, 1325 m of altitude). *Earth System Science Data*, *11*(1), 71–88. https://doi.org/10.5194/essd-11-71-2019

Liu, X., & Chen, B. (2000). Climatic warming in the Tibetan Plateau during recent decades. *International Journal of Climatology*, *20*(14), 1729–1742. https://doi.org/10.1002/1097-0088(20001130)20:14<1729::AID-JOC556>3.0.CO;2-Y

Liu, X., Cheng, Z., Yan, L., & Yin, Z. Y. (2009). Elevation dependency of recent and future minimum surface air temperature trends in the Tibetan Plateau and its surroundings. *Global and Planetary Change*, *68*(3), 164–174. https://doi.org/10.1016/j.gloplacha.2009.03.017

López-Moreno, J. I. (2005). Recent variations of snowpack depth in the central Spanish Pyrenees. *Arctic, Antarctic, and Alpine Research*, *37*(2), 253–260. https://doi.org/10.1657/1523-0430(2005)037[0253:RVOSDI]2.0.CO;2

Mao, Y., Nijssen, B., & Lettenmaier, D. P. (2015). Is climate change implicated in the 2013-2014 California drought? A hydrologic perspective. *Geophysical Research Letters*, *42*(8), 2805–2813. https://doi.org/10.1002/2015GL063456

Masson, D., & Frei, C. (2016). Long-term variations and trends of mesoscale precipitation in the Alps: recalculation and update for 1901-2008. *International Journal of Climatology*, *36*(1), 492–500. https://doi.org/10.1002/joc.4343

Nepal, S. (2016). Impacts of climate change on the hydrological regime of the Koshi river basin in the Himalayan region. *Journal of Hydro-Environment Research*, *10*, 76–89. https://doi.org/10.1016/j.jher.2015.12.001

Ohmura, A. (2012). Enhanced temperature variability in high-altitude climate change. *Theoretical and Applied Climatology*, *110*(4), 499–508. https://doi.org/10.1007/s00704-012-0687-x

Oyler, J. W., Dobrowski, S. Z., Ballantyne, A. P., Klene, A. E., & Running, S. W. (2015). Artificial amplification of warming trends across the mountains of the western United States. *Geophysical Research Letters*, *42*(1), 153–161. https://doi.org/10.1002/2014GL062803

Palazzi, E., von Hardenberg, J., & Provenzale, A. (2013). Precipitation in the Hindu-Kush Karakoram Himalaya: Observations and future scenarios. *Journal of Geophysical Research: Atmospheres*, *118*(1), 85–100. https://doi.org/10.1029/2012JD018697

Panday, P. K., Thibeault, J., & Frey, K. E. (2015). Changing temperature and precipitation extremes in the Hindu Kush-Himalayan region: an analysis of CMIP3 and CMIP5 simulations and projections. *International Journal of Climatology*, *35*(10), 3058–3077. https://doi.org/10.1002/joc.4192

Pepin, N. C., & Lundquist, J. D. (2008). Temperature trends at high elevations: Patterns across the globe. *Geophysical Research Letters*, *35*(14), 1–6. https://doi.org/10.1029/2008GL034026

Pepin, N. C., & Seidel, D. J. (2005). A global comparison of surface and free-air temperatures at high elevations. *Journal of Geophysical Research D: Atmospheres*, *110*(3), 1–15. https://doi.org/10.1029/2004JD005047

Pérez-Zanón, N., Sigró, J., & Ashcroft, L. (2017). Temperature and precipitation regional climate series over the central Pyrenees during 1910-2013. *International Journal of Climatology*, *37*(4), 1922–1937. https://doi.org/10.1002/joc.4823

Qin, J., Yang, K., Liang, S., & Guo, X. (2009). The altitudinal dependence of recent rapid warming over the Tibetan Plateau. *Climatic Change*, *97*(1), 321–327. https://doi.org/10.1007/s10584-009-9733-9

Qixiang, W., Wang, M., & Fan, X. (2018). Seasonal patterns of warming amplification of high-elevation stations across the globe. *International Journal of Climatology*, *38*(8), 3466–3473. https://doi.org/10.1002/joc.5509

Rottler, E., Kormann, C., Francke, T., & Bronstert, A. (2019). Elevation-dependent warming in the Swiss Alps 1981–2017: Features, forcings and feedbacks. *International Journal of Climatology*, *39*(5), 2556–2568. https://doi.org/10.1002/joc.5970

Ruiz, D., Moreno, H. A., Gutiérrez, M. E., & Zapata, P. A. (2008). Changing climate and endangered high mountain ecosystems in Colombia. *Science of The Total Environment*, *398*(1–3), 122–132. https://doi.org/10.1016/j.scitotenv.2008.02.038

Rusticucci, M., Zazulie, N., & Raga, G. B. (2014). Regional winter climate of the southern central Andes: Assessing the performance of ERA-Interim for climate studies. *Journal of Geophysical Research: Atmospheres*, *119*(14), 8568–8582. https://doi.org/10.1002/2013JD021167

Salerno, F., Guyennon, N., Thakuri, S., Viviano, G., Romano, E., Vuillermoz, E., et al. (2015). Weak precipitation, warm winters and springs impact glaciers of south slopes of Mt. Everest (central Himalaya) in the last 2 decades (1994–2013). *The Cryosphere*, *9*(3), 1229–1247. https://doi.org/10.5194/tc-9-1229-2015

Scherrer, S. C., Ceppi, P., Croci-Maspoli, M., & Appenzeller, C. (2012). Snow-albedo feedback and Swiss spring temperature trends. *Theoretical and Applied Climatology*, *110*(4), 509–516. https://doi.org/10.1007/s00704-012-0712-0

Schmocker, J., Liniger, H. P., Ngeru, J. N., Brugnara, Y., Auchmann, R., & Brönnimann, S. (2016). Trends in mean and extreme precipitation in the Mount Kenya region from observations and reanalyses. *International Journal of Climatology*, *36*(3), 1500–1514. https://doi.org/10.1002/joc.4438

Scorzini, A. R., & Leopardi, M. (2019). Precipitation and temperature trends over central Italy (Abruzzo Region): 1951–2012. *Theoretical and Applied Climatology*, *135*(3–4), 959–977. https://doi.org/10.1007/s00704-018-2427-3

Spinoni, J., Szalai, S., Szentimrey, T., Lakatos, M., Bihari, Z., Nagy, A., et al. (2015). Climate of the Carpathian Region in the period 1961-2010: climatologies and trends of 10 variables. *International Journal of Climatology*, *35*(7), 1322–1341. https://doi.org/10.1002/joc.4059

Tudoroiu, M., Eccel, E., Gioli, B., Gianelle, D., Schume, H., Genesio, L., & Miglietta, F. (2016). Negative elevation-dependent warming trend in the Eastern Alps. *Environmental Research Letters*, *11*(4), 044021. https://doi.org/10.1088/1748-9326/11/4/044021

Vincent, L. A., Zhang, X., Brown, R. D., Feng, Y., Mekis, E., Milewska, E. J., et al. (2015). Observed Trends in Canada's Climate and Influence of Low-Frequency Variability Modes. *Journal of Climate*, *28*(11), 4545–4560. https://doi.org/10.1175/JCLI-D-14-00697.1

Vuille, M., Franquist, E., Garreaud, R., Lavado Casimiro, W. S., & Cáceres, B. (2015). Impact of the global warming hiatus on Andean temperature. *Journal of Geophysical Research: Atmospheres*, *120*(9), 3745–3757. https://doi.org/10.1002/2015JD023126

Wendler, G., Gordon, T., & Stuefer, M. (2017). On the Precipitation and Precipitation Change in Alaska. *Atmosphere*, *8*(12), 253. https://doi.org/10.3390/atmos8120253

Xu, F., Jia, Y., Peng, H., Niu, C., & Liu, J. (2018). Temperature and precipitation trends and their links with elevation in the Hengduan Mountain region, China. *Climate Research*, *75*(2). https://doi.org/10.3354/cr01516

Yan, L., & Liu, X. (2014). Has Climatic Warming over the Tibetan Plateau Paused or Continued in Recent Years ? *Journal of Earth, Ocean and Atmospheric Sciences*, *1*(1), 13–28.

You, Q., Kang, S., Pepin, N., Flügel, W. A., Yan, Y., Behrawan, H., & Huang, J. (2010). Relationship between temperature trend magnitude, elevation and mean temperature in the Tibetan Plateau from homogenized surface stations and reanalysis data. *Global and Planetary Change*, *71*(1–2), 124–133. https://doi.org/10.1016/j.gloplacha.2010.01.020

Zazulie, N., Rusticucci, M., & Raga, G. B. (2017). Regional climate of the subtropical central Andes using high-resolution CMIP5 models—part I: past performance (1980–2005). *Climate Dynamics*, *49*(11–12), 3937–3957. https://doi.org/10.1007/s00382-017-3560-x

Zeng, Z., Chen, A., Ciais, P., Li, Y., Li, L. Z. X., Vautard, R., et al. (2015). Regional air pollution brightening reverses the greenhouse gases induced warming-elevation relationship. *Geophysical Research Letters*, *42*(11), 4563–4572. https://doi.org/10.1002/2015GL064410

Zhang, D., Yang, Y., & Lan, B. (2018). Climate variability in the northern and southern Altai Mountains during the past 50 years. *Scientific Reports*, *8*(1), 3238. https://doi.org/10.1038/s41598-018-21637-x

		Global	Andes	Tibet	GAR	Rockies
CRU	1900-2018	1.02/0.95/0.06**	0.34/0.33/0.01	0.79/1.04/-0.24**	1.46/1.44/0.03*	1.05/0.93/0.12
	1940-2018	1.50/1.50/0.00	0.43/0.52/-0.08	1.16/1.55/-0.39**	2.13/2.15/-0.02	1.49/1.28/0.20
	1960-2018	2.37/2.27/0.09	0.67/0.63/0.03	2.15/2.32/-0.17	3.36/3.39/-0.03	2.26/2.11/0.16
	1980-2018	2.75/2.61/0.14	0.47/1.24/-0.78**	2.73/2.81/-0.08	4.51/4.66/-0.15*	2.88/2.20/0.69
GISTEMP	1900-2018	1.13/1.13/-0.01	?/1.25/?	1.06/1.11/-0.05	1.28/1.18/0.10**	1.02/0.84/0.19
	1940-2018	1.68/1.68/0.00	1.24/1.30/-0.07	1.42/1.61/-0.20**	1.99/1.88/0.11**	1.69/1.34/0.35
	1960-2018	2.59/2.45/0.14	1.53/1.60/-0.07	2.43/2.53/-0.10	3.23/3.08/0.15**	2.59/2.20/0.39
	1980-2018	3.01/2.78/0.23	1.30/1.36/-0.06	3.11/3.16/-0.05	4.54/4.33/0.21**	3.16/2.12/1.04
ERA5	1980-2018	3.32/3.06/0.27*	2.08/1.94/0.14	3.29/3.00/0.29	5.37/4.44/0.93**	3.66/2.45/1.21*
CMIP5	1900-2018	0.84/0.83/0.02	0.78/0.67/0.11**	0.73/0.72/0.01	0.72/0.71/0.01*	0.74/0.71/0.03
	1940-2018	1.30/1.24/0.06	1.06/0.91/0.15**	1.17/1.15/0.02	1.27/1.28/-0.01	1.24/1.13/0.11*
	1960-2018	2.42/2.26/0.16**	1.89/1.69/0.20**	2.34/2.27/0.06*	2.55/2.55/0.00	2.48/2.35/0.13
	1980-2018	3.88/3.42/0.46**	2.38/2.12/0.26**	3.93/3.73/0.19**	4.18/4.13/0.05*	4.27/4.35/-0.08

Table S2. Temperature trends (°C/100y) for mountain/lowland/elevation gradient by region for four different periods using four different global gridded datasets (mountain regions defined by boxes in Figure 1). Trend figures show mountain warming rate/lowland warming rate/rate of change in elevation gradient. All absolute trends are positive (warming). Red = mountain warming significantly faster than lowlands. Pink = mountain warming faster (not-significant). Light Orange = mountain warming slower (not significant), Dark Orange = mountain warming significantly slower. Significance of trend in the difference is based on the Mann Kendal test **p<0.01, *p<0.05.

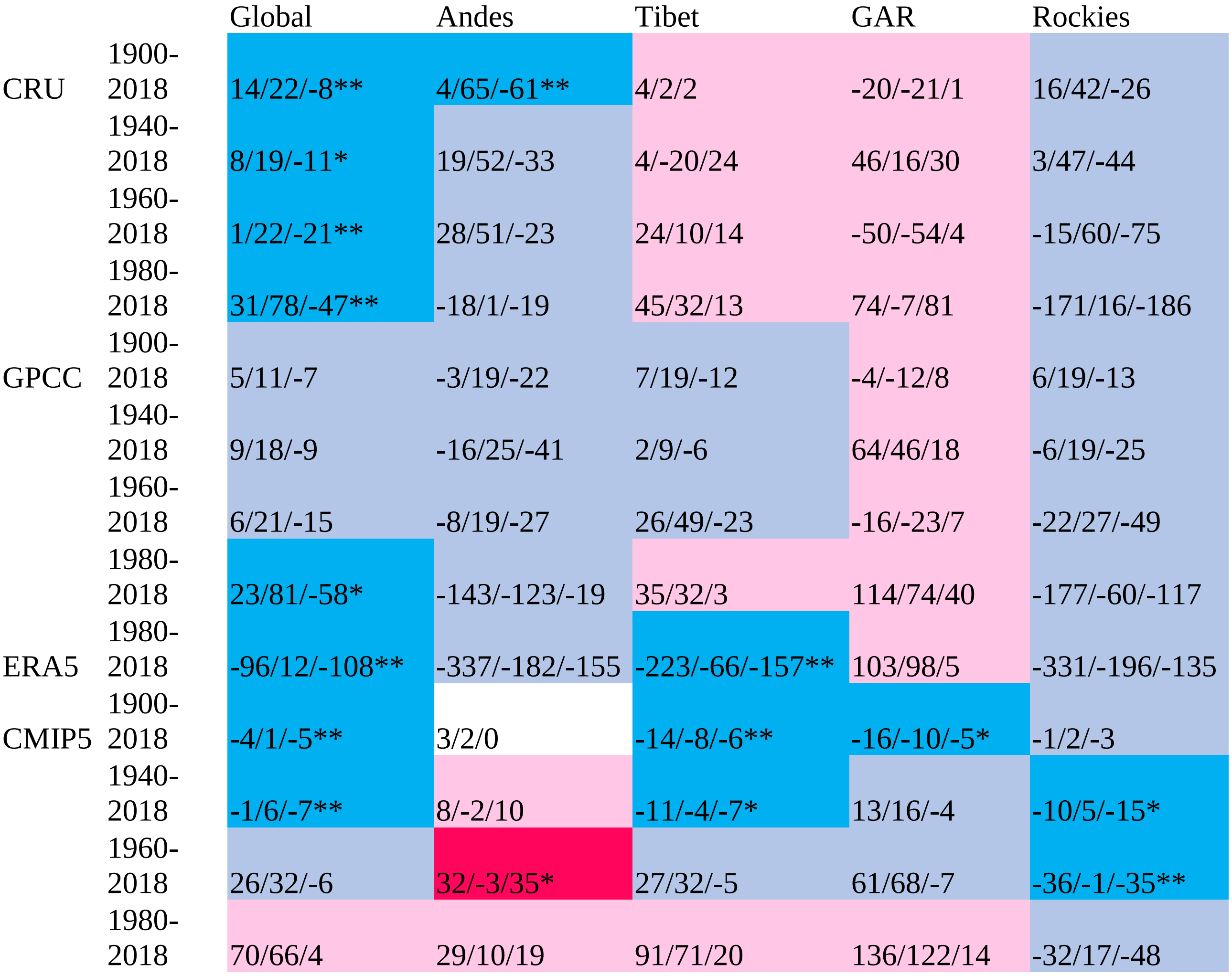

		Global	Andes	Tibet	GAR	Rockies
CRU	1900-2018	14/22/-8**	4/65/-61**	4/2/2	-20/-21/1	16/42/-26
	1940-2018	8/19/-11*	19/52/-33	4/-20/24	46/16/30	3/47/-44
	1960-2018	1/22/-21**	28/51/-23	24/10/14	-50/-54/4	-15/60/-75
	1980-2018	31/78/-47**	-18/1/-19	45/32/13	74/-7/81	-171/16/-186
GPCC	1900-2018	5/11/-7	-3/19/-22	7/19/-12	-4/-12/8	6/19/-13
	1940-2018	9/18/-9	-16/25/-41	2/9/-6	64/46/18	-6/19/-25
	1960-2018	6/21/-15	-8/19/-27	26/49/-23	-16/-23/7	-22/27/-49
	1980-2018	23/81/-58*	-143/-123/-19	35/32/3	114/74/40	-177/-60/-117
ERA5	1980-2018	-96/12/-108**	-337/-182/-155	-223/-66/-157**	103/98/5	-331/-196/-135
CMIP5	1900-2018	-4/1/-5**	3/2/0	-14/-8/-6**	-16/-10/-5*	-1/2/-3
	1940-2018	-1/6/-7**	8/-2/10	-11/-4/-7*	13/16/-4	-10/5/-15*
	1960-2018	26/32/-6	32/-3/35*	27/32/-5	61/68/-7	-36/-1/-35**
	1980-2018	70/66/4	29/10/19	91/71/20	136/122/14	-32/17/-48

Table S3. Trends for mountain precipitation/lowland precipitation/orographic precipitation gradient for individual mountain regions and adjacent lowlands (defined by boxes in Figure 1). Red = significant increased orographic gradient. Pink = increased orographic gradient (not-significant). Light Blue = decreased orographic gradient (not significant). Dark Blue = significant decreased orographic gradient. Significance of trend in the difference is based on the Mann Kendal test **p<0.01, *p<0.05.